Optik 126 (2015) 1181–1184

Contents lists available at ScienceDirect

Optik

journal homepage: www.elsevier.de/ijleo

Core field analysis of elliptical Bragg fibers

Xinbo Chou, Huajun Yang*, Hualie Jiang, Jiang Wu, Ping Jiang

School of Physical Electronics, University of Electronic Science and Technology of China, Chengdu 610054, China

ARTICLE INFO

Article history:
Received 19 February 2014
Accepted 3 March 2015

Keywords:
Elliptical Bragg fibers
Propagation constant
Core energy flux

ABSTRACT

The propagation constant expression and the field distribution by employing the boundary conditions and QWS condition have been derived. The longitudinal and azimuthal fields have been discussed by the simulation method. We have mainly analyzed the HE_{11} mode and figured out the guided flux of the core. By comparing the energy flux of different eccentricity situations, we obtain that the circular waveguide theory may be a particular case of the elliptical one. The process of ellipse tends to split the field into parts, which are in direct proportion to the mode orders.

1. Introduction

The concept of Bragg fiber was first proposed in the classic paper by Yeh et al. at 1978 [1]. Compared with conventional optical fibers, Bragg fibers possess a different propagation principle by the bandgap (PBG) effect and very innovative characteristics, such as the low propagation loss [2–4]. However, in most cases, it is difficult to make perfect cylindrical Bragg fibers and other factors may also distort the shape [5], usually into a ellipse-like one. So we have analyzed the characteristics of elliptical Bragg fibers in this paper.

2. Derivation of propagation constant and electromagnetic field

The structure of elliptical Bragg fibers is shown in Fig. 1. The elliptical Bragg fiber consists of a low-index elliptical core surrounded by high and low-refractive-index layers.

The transverse refractive index distribution of elliptical Bragg fibers is:

$$n(\xi)=\begin{cases} n_c, & 0<\xi<\xi_1 \\ n_1, & \xi_{2v-1}<\xi<\xi_{2v} \\ n_2, & \xi_{2v}<\xi<\xi_{2v+1} \\ & \dots \end{cases} \tag{1}$$

where $v = 1, 2, 3, \dots, \infty$.

It is convenient to analyze it in the elliptic coordinate system, shown as Fig. 2.

In terms of the rectangular coordinates (x,y,z), the elliptical cylinder coordinates (ξ,η,z') are defined as follows:

$$\begin{aligned} x &= c\ \cosh(\xi)\cos(\eta) \\ y &= c\ \sinh(\xi)\sin(\eta) \\ z &= z' \end{aligned} \tag{2}$$

where c is foci of the core and the eccentricity $e = 1/(\cosh(\xi_0))$. The solution of axial fields of the wave equation in elliptical cylindrical system satisfies

$$\left[\frac{1}{c^2\left(\sqrt{\sinh^2\xi+\sin^2\eta}\right)}\left(\frac{\partial}{\partial^2\xi}+\frac{\partial}{\partial^2\eta}\right)+p^2\right]\begin{bmatrix}E_Z\\H_Z\end{bmatrix}=0 \tag{3}$$

where $p^2 = k_i^2 - \beta^2$, $k_i^2 = \omega^2\mu_i\varepsilon_i$. The transverse field components can be derived from the axial fields as follows:

$$\begin{aligned} E_\xi &= \frac{-j}{cp^2\sqrt{(\sinh^2\xi+\sin^2\eta)}}\left(\beta\frac{\partial E_Z}{\partial\xi}+\omega\mu\frac{\partial H_Z}{\partial\eta}\right) \\ H_\xi &= \frac{-j}{cp^2\sqrt{(\sinh^2\xi+\sin^2\eta)}}\left(\beta\frac{\partial H_Z}{\partial\xi}-\omega\varepsilon\frac{\partial E_Z}{\partial\eta}\right) \\ E_\eta &= \frac{-j}{cp^2\sqrt{(\sinh^2\xi+\sin^2\eta)}}\left(\beta\frac{\partial E_Z}{\partial\eta}-\omega\mu\frac{\partial H_Z}{\partial\xi}\right) \\ H_\eta &= \frac{-j}{cp^2\sqrt{(\sinh^2\xi+\sin^2\eta)}}\left(\beta\frac{\partial H_Z}{\partial\eta}+\omega\varepsilon\frac{\partial E_Z}{\partial\xi}\right) \end{aligned} \tag{4}$$

* Corresponding author. Tel.: +0086 13880880789.
E-mail address: yanghj@uestc.edu.cn (H. Yang).

http://dx.doi.org/10.1016/j.ijleo.2015.03.023

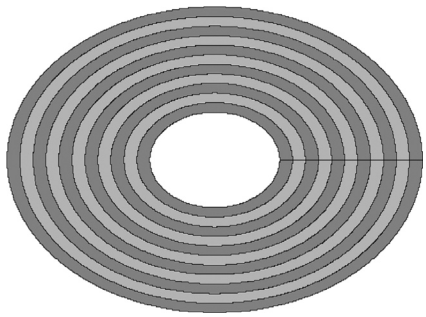

Fig. 1. Structure of elliptical Bragg fiber.

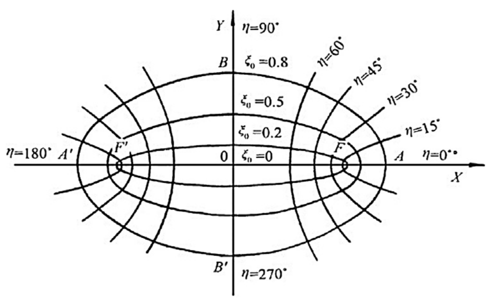

Fig. 2. The elliptic coordinate system.

By using the separation method, that is, $E_z(\xi,\eta) = R(\xi)\Phi(\eta)$ from Eq. (3), we can get:

$$\frac{d^2\Phi}{d^2\eta} + (\lambda - 2q\cos 2\eta)\Phi(\eta) = 0 \quad (5)$$

$$\frac{d^2R}{d^2\xi} - (\lambda - 2q\cosh 2\xi)R(\xi) = 0 \quad (6)$$

With $q = c^2(p^2 - \beta^2)/4$, so it is the same with H_z.

The solution of Eq. (3) consists of radial and angular Mathieu functions. There are two orientations for the field in elliptical fibers. Without losing the generality, here we consider the HE mode only. In Bragg fibers, the propagation satisfies $0 \le \beta/\kappa_0 \le n_c$. Then, at a general cladding interface $\xi = \xi_0$, the axial electromagnetic field can be expressed as

$$\begin{cases} H_{Z0} = A_m Ce_m(\xi, q_0) ce_m(\eta, q_0) \\ E_{z0} = B_m Se_m(\xi, q_0) se_m(\eta, q_0) \end{cases} \quad (0 < \xi < \xi_0) \quad (7)$$

and

$$\begin{cases} H_{Z1} = C_m Fey_m(\xi, q_1) ce_m(\eta, q_1) \\ E_{z1} = D_m Gey_m(\xi, q_1) se_m(\eta, q_1) \end{cases} \quad (\xi_0 < \xi < \infty) \quad (8)$$

where Ce, Se, Fey, Gey are radial Mathieu functions of the first and second kind and ce, se are the angular Mathieu functions of the first kind in accordance with Ref. [6].

According to the boundary conditions, we obtain:

$$\begin{cases} H_{Z0} = H_{Z1} \\ E_{Z0} = E_{Z1} \\ H_{\eta 0} = H_{\eta 1} \\ E_{\eta 0} = E_{\eta 1} \end{cases} \quad (9)$$

The eigenvalue equation of propagation constant can be obtained:

$$\frac{\kappa_1^2}{\beta^2}\left(n_c \frac{b'_m}{b_m} + \frac{q_0}{q_1} n_1 \frac{d'_m}{d_m}\right)\left(\frac{1}{n_c}\frac{a'_m}{a_m} + \frac{q_0}{n_1 q_1}\frac{c'_m}{c_m}\right) + \left(X_{mm} + \frac{q_0}{q_1}\frac{W_{mm}}{\alpha_{mm}}\right)\left(V_{mm} + \frac{q_0}{q_1}\frac{\theta_{mm}}{\beta_{mm}}\right) = 0 \quad (10)$$

$$\begin{aligned} a_m &= Ce_m(\xi_0, q_0), \quad a'_m = \left[\frac{dCe_m(\xi, q_0)}{d\xi}\right]_{\xi=\xi_0} \\ b_m &= Se_m(\xi_0, q_0), \quad b'_m = \left[\frac{dSe_m(\xi, q_0)}{d\xi}\right]_{\xi=\xi_0} \\ c_m &= Fey_m(\xi_0, q_1), \quad c'_m = \left[\frac{dFey_m(\xi, q_1)}{d\xi}\right]_{\xi=\xi_0} \\ d_m &= Gey_m(\xi_0, q_1), \quad d'_m = \left[\frac{dGey_m(\xi, q_1)}{d\xi}\right]_{\xi=\xi_0} \end{aligned} \quad (11)$$

$$\begin{aligned} \alpha_{mm} &= \frac{\int_0^{2\pi} ce_m(\eta, q_1) ce_m(\eta, q_0) d\eta}{\pi} \\ \beta_{mm} &= \frac{\int_0^{2\pi} se_m(\eta, q_1) se_m(\eta, q_0) d\eta}{\pi} \\ X_{mm} &= \frac{\int_0^{2\pi} se_m(\eta, q_0) ce'_m(\eta, q_0) d\eta}{\pi} \\ W_{mm} &= \frac{\int_0^{2\pi} ce'_m(\eta, q_1) se_m(\eta, q_0) d\eta}{\pi} \\ V_{mm} &= \frac{\int_0^{2\pi} se_m(\eta, q_0) ce_m(\eta, q_0) d\eta}{\pi} \\ \theta_{mm} &= \frac{\int_0^{2\pi} se'_m(\eta, q_1) ce_m(\eta, q_0) d\eta}{\pi} \end{aligned} \quad (12)$$

These coefficients will be obtained by Simpson's Integral Method.

3. Analysis about the results

Here we suppose that $\xi_0 = 1$, $n_c = 1$, $n_1 = 1.58$, the major axis of the core $a = 10^{-6}m$. As we know, $E_{z0} = 0$ at $\xi = \xi_0$, that is to say, for HE mode $Se_m(\xi_0, q) = 0$.

Let $m = 1$, we get the first few parametric values of HE modes $q_{1,1} = 2.37185$, $q_{1,2} = 8.22379$. The E_Z field structure of $HE_{1,1}$ is shown in Fig. 3 and $HE_{1,2}$ in Fig. 4.

From the two figures, we can see that $HE_{m,n}$ mode has m angular nodal lines and n radial nodal lines including the boundary line. And the E_η field structure of $HE_{1,2}$, $HE_{2,1}$, $HE_{2,2}$ are shown in Figs. 5–7.